NUKLEONIKA 2004;49(Supplement 2):S67–S70

PROCEEDINGS

Pion interferometry in Au+Au collisions at $\sqrt{s_{NN}} = 200$ GeV

Mercedes López Noriega

for the STAR Collaboration

Abstract We present preliminary results from a two-pion intensity interferometry analysis from Au+Au collisions at $\sqrt{s_{NN}} =$ 200 GeV measured in the STAR detector at RHIC. The dependence of the apparent pion source on multiplicity and transverse momentum are discussed and compared with preliminary results from d+Au and p+p collisions at the same beam energy.

Key words STAR • RHIC • HBT • interferometry • pion

Introduction

Two particle intensity interferometry (HBT) is a useful tool to study the space-time geometry of the particle emitting source in heavy ion collisions [6, 9]. It also contains dynamical information that can be explored by studying the transverse momentum dependence of the apparent source size [13, 14]. Extracted parameters in HBT analysis from Au+Au collisions at $\sqrt{s_{NN}} = 130$ GeV at the Relativistic Heavy Ion Collider (RHIC) did not agree with predictions of hydrodynamic models that gave an almost perfect description of the momentum-space structure of the emitting source and elliptic flow [10]. This HBT puzzle could originate from the fact that the extracted timescales (emission duration from the R_o/R_s ratio and evolution duration from the m_T dependence of R_l) are smaller than those predicted by the hydrodynamical model [10].

In this paper we present two-pion correlation systematics as a function of the transverse total mass ($m_T = \sqrt{k_T^2 + m^2}$, $\mathbf{k}_T = ½(\mathbf{p}_1 + \mathbf{p}_2)_T$) and multiplicity in Au+Au collisions at $\sqrt{s_{NN}} = 200$ GeV produced by RHIC at Brookhaven National Laboratory and measured by the STAR detector. We also discuss a fitting procedure in which the strength of the final state Coulomb interaction between the two charged pions is taking into account in the fit itself.

Experimental details

Experimentally, two-particle correlations are studied by constructing the correlation function $C_2(\mathbf{q}) = A(\mathbf{q})/B(\mathbf{q})$. Here $A(\mathbf{q})$ is the measured distribution of the momentum difference $\mathbf{q} = \mathbf{p}_1 - \mathbf{p}_2$ for pairs of particles from the same event, and $B(\mathbf{q})$ is the corresponding distribution for pairs of particles from different events. For this analysis we selected events with a collision vertex position within ±25 cm measured from the center of the 4 m long STAR Time Projection Chamber (TPC), and we mixed events only if their longitudinal primary vertex positions were no

M. López Noriega
The Ohio State University,
174 W 18th Ave., Columbus, Ohio 43210, USA,
Tel.: +1 614 292 5321, Fax: +1 614 292 7557,
e-mail: mercedes@pacific.mps.ohio-state.edu

Received: 25 January 2004

further apart than 5 cm. We divided our sample into six centrality bins, where the centrality was characterized according to the measured multiplicity of charged particles at midrapidity. The six centrality bins correspond to 0–5% (most central), 5–10%, 10–20%, 20–30%, 30–50% and 50–80% (most peripheral) of the total hadronic cross section. Charged pions were identified by correlating their specific ionization in the gas of the TPC with their measured momentum [1].

The effects of track-splitting (reconstruction of a single track as two tracks) and track-merging (two tracks with similar momenta reconstructed as a single track) were eliminated as described in [5]. A new procedure to take into account final state Coulomb interaction is described in the next section.

The effect of the single-particle momentum resolution ($\delta p/p \sim 1\%$ for pions) induces systematic underestimation of the HBT parameters. Using an iterative procedure [5], we corrected our correlation functions for finite resolution effects. The correction due to the uncertainty on the removal of the artificial reduction of the HBT parameters associated with the anti-merging cut has been calculated in [3] and is included as systematic error.

Fitting procedure

The three-dimensional correlation functions were generated. The relative momentum was measured in the longitudinal co-moving system (LCMS) frame, and decomposed according to the Pratt-Bertsch [7, 15] out-side-long parametrization. There is a Coulomb interaction between emitted particles that needs to be taken into account in order to isolate the Bose-Einstein interaction. This Coulomb interaction, repulsive for like-sign particles, causes a reduction on the number of real pairs at low q, reducing the correlation function. In our previous analysis [5, 12] as well as in previous experiments, this was corrected by applying a pair Coulomb correction to each pair in the background [15] corresponding to a spherical Gaussian source of a given radius; we call this standard procedure. The correlation function was then fit with the functional form:

$$(1)\quad C(q_o,q_s,q_l)=\frac{\mathrm{A}(\mathbf{q})}{\mathrm{B}(\mathbf{q})\times K_{coul}(q_{inv})} = 1+\lambda\exp\left(-R_o^2q_o^2-R_s^2q_s^2-R_l^2q_l^2\right)$$

where $K_{coul}(q_{inv})$ is the square of the Coulomb wave-function. However, this procedure overcorrects the correlation function since all background pairs are corrected, including those that are not formed by primary pions.

We have implemented a new procedure, first suggested by Bowler [8] and Sinyukov [17] and recently used by the CERES collaboration [2], in which the strength of the Coulomb interaction is taken into account in the fit itself and only pairs with Bose-Einstein interaction are considered to Coulomb interact; we call this Bowler-Sinyukov procedure. The fit in this case is:

$$(2)\quad C(q_o,q_s,q_l)=\frac{\mathrm{A}(\mathbf{q})}{\mathrm{B}(\mathbf{q})}=(1-\lambda) + \lambda K_{coul}(q_{inv})\left(1+\exp\left(-R_o^2q_o^2-R_s^2q_s^2-R_l^2q_l^2\right)\right)$$

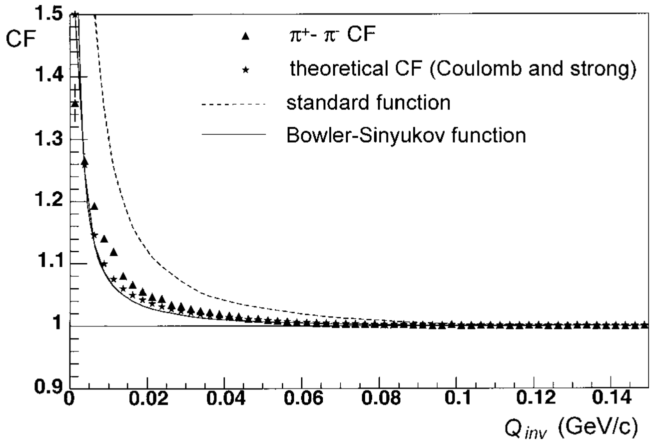

Fig. 1. Experimental (triangles) and theoretical [11] (stars) 1D $\pi^+\pi^-$ correlation functions compared with standard (discontinuous line) and Bowler-Sinyukov (continuous line) functions.

where $K_{coul}(q_{inv})$ is the same as above. In Fig. 1, the measured $\pi^+\pi^-$ correlation function is compared to several calculations. Lines indicate the standard ($K_{coul}(q_{inv})$) and Bowler-Sinyukov ($1 + (\lambda - 1)K_{coul}(q_{inv})$) Coulomb functions; in the latter, λ was extracted from the fit to the 3D like-sign correlation function. Clearly, the Bowler-Sinyukov function better reproduces the data. Further improvement is observed when the strong interaction (negligible for like-sign pion correlations) is included [11] into the $\pi^+\pi^-$ final state interactions.

When we use this procedure in our 3D analysis we observe an increase in R_o of 10–15%. The values of R_s and R_l do not depend significantly on the Coulomb procedure. Consequently the increase in R_o/R_s is not enough to solve the HBT puzzle.

HBT parameters *vs.* centrality and transverse momentum

Figure 2 shows the m_T dependence of the source parameters for pions at six centrality bins from Au+Au collisions as well as from p+p and d+Au collisions at same beam energy. The three radii increase with increasing centrality and R_l varies similar to R_o and R_s; for R_o and R_s this increase may be attributed to the geometrical overlap of the two nuclei. The extracted radii rapidly decrease as a function of m_T, which is an indication of transverse flow [18]. In order to extract information about the m_T dependence on centrality, we fit the m_T dependence of each radius and each centrality to a power-law function: $R_i(m_T) = R_{i0} \times (m_T/m_\pi)^{-\alpha}$ (solid lines in Fig. 2). Figure 3 shows the dependence of α on the number of participants; for Au+Au, α is constant for R_l as a function of number of participants and decreases with the number of participants for R_o and R_s for the most peripheral bins indicating a decrease of transverse flow for these collisions. $R_o/R_s \sim 1$ which indicates a short emission duration in a blast wave fit [16].

Assuming boost-invariant longitudinal flow we can extract an evolution time-scale by using a simple fit [16]:

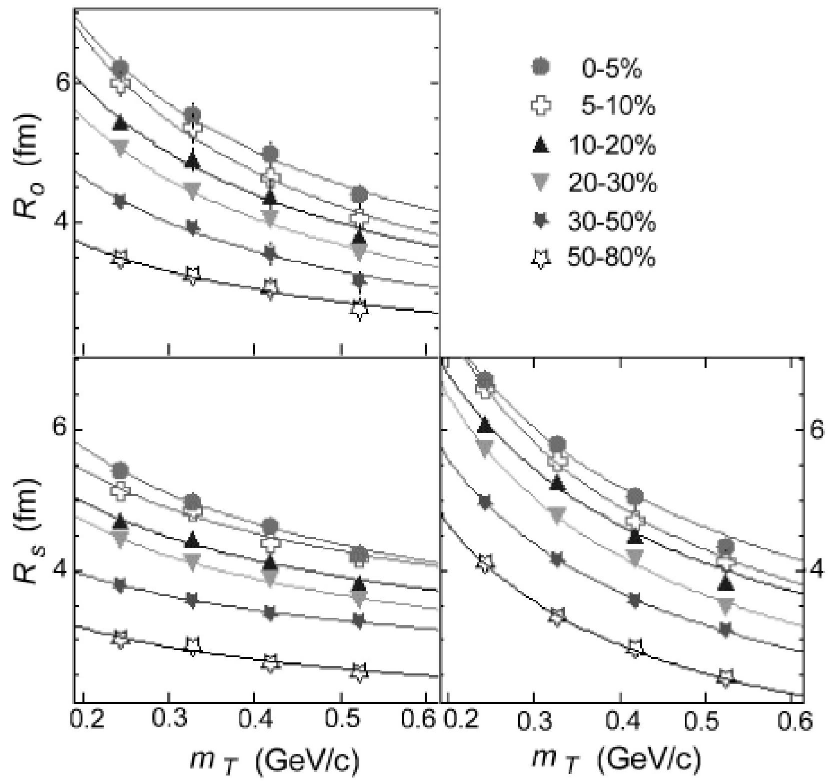

Fig. 2. HBT radii for 6 different centrality from Au+Au collisions, and from p+p and d+Au collisions. The lines indicate power-law fits to each parameter and centrality.

(3) $$R_l = \langle t_{fo} \rangle \sqrt{\frac{T}{m_T} \frac{K_2(m_T/T)}{K_1(m_T/T)}}$$

where T is the freeze-out temperature and K_1 and K_2 are the modified Bessel functions of order 1 and 2. For T extracted from fits to pion, kaon, and proton transverse momentum spectra (90 MeV for most central and 120 MeV for most peripheral collisions) [4] we get $<t_{fo}> \approx 9$ fm/c for central events and $<t_{fo}> \approx 6$ fm/c for peripheral events. Hence, the evolution time, in addition to the emission duration, is quite short.

For a transverse expanding, longitudinally boost-invariant source, and assuming a Gaussian transverse density profile, we can extract information about its radius, R_{geom}, by fitting the m_T dependence of R_s to:

(4) $$R_s = (m_T) = \sqrt{\frac{R_{geom}^2}{1 + \eta_f^2 \left(\frac{1}{2} + \frac{m_T}{T} \right)}}$$

where T is again the freeze-out temperature and η_f is the surface transverse rapidity [19]. For T and η_f consistent with spectra we see an increase on this radius from ~5 fm for the most peripheral case to ~13 fm for the most central one as shown in Fig. 4. We also observe a smooth transition from p+p ($N_{participants}$ = 2) and d+Au ($N_{participants}$ = 8.3) to Au+Au collisions.

Conclusion

We have presented identical pion interferometry results for Au+Au collisions at $\sqrt{s_{NN}}$ = 200 GeV. With respect to multiplicity and m_T dependencies, pion HBT radii are very similar to results reported at $\sqrt{s_{NN}}$ = 130 GeV. HBT radii and geometrical radius increase with increasing centrality. HBT radii decrease with m_T and we observe a stronger flow for the most central collisions. Our results indicate that both the evolution time-scale (as measured by the m_T

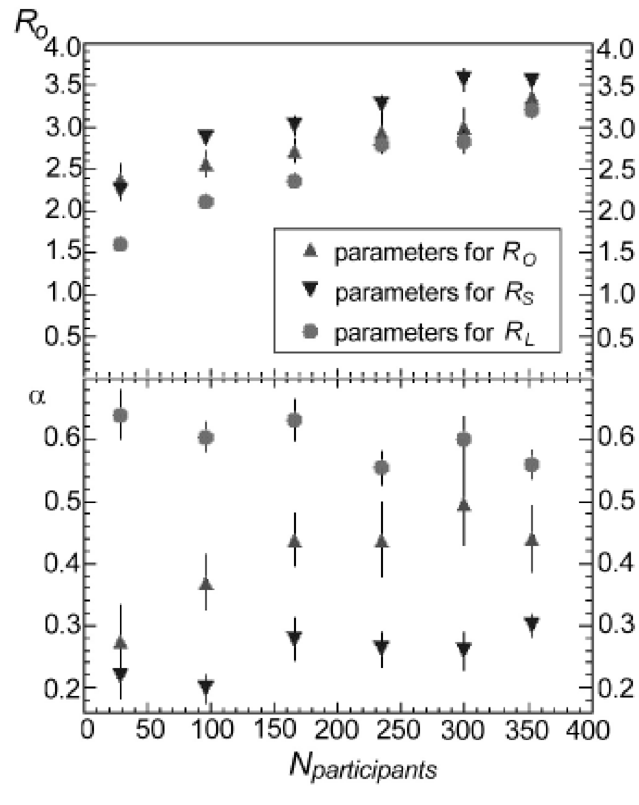

Fig. 3. Extracted α parameter from the power-law fits to the HBT radii (lines in Fig. 2) for p+p, d+Au and 6 different centralities in Au+Au collisions.

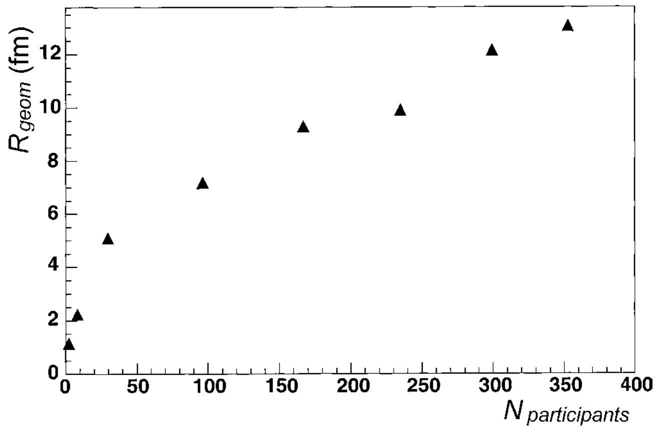

Fig. 4. Extracted R_{geom} radius for a transverse Gaussian density profile [19] for p+p, d+Au and 6 different centralities in Au+Au collisions.

dependence of R_l) and the emission duration (probed by comparing R_o to R_s) are surprisingly fast. The Bowler-Sinyukov Coulomb procedure does not solve the HBT puzzle although increases the ratio R_o/R_s by 10–15%.

References

1. Ackermann KH (for the STAR Collaboration) (2003) STAR detector overview. Nucl Instrum Meth Phys Res A 499:624–632
2. Adamova D (for the CERES Collaboration) (2003) Beam energy and centrality dependence of two-pion Bose-Einstein correlations at SPS energies. Nucl Phys A 714:124–144
3. Adams J (for the STAR Collaboration) (2004) Azimuthally sensitive HBT in Au+Au collisions at s(NN)**(1/2) = 200 GeV. Phys Rev Lett 93:012301–012307
4. Adams J (for the STAR Collaboration) (2004) Identified particle distributions in pp and Au+Au collisions at s(NN)**(1/2) = 200 GeV. Phys Rev Lett 92:112301–112307
5. Adler C (for the STAR Collaboration) (2001) Pion interferometry of s(NN)**(1/2) = 130 GeV Au+Au collisions at RHIC. Phys Rev Lett 87:082301–082307
6. Bauer W, Gelbke CK, Pratt S (1992) Hadronic interferometry in heavy ion collisions. Annu Rev Nucl Part Sci 42:77–100
7. Bertsch G (1989) Pion interferometry as a probe of the plasma. Nucl Phys A 498:173c–180c
8. Bowler MG (1991) Coulomb corrections to Bose-Einstein correlations have been greatly exaggerated. Phys Lett B 270:69–74
9. Heinz U, Jacak B (1999) Two-particle correlations in relativistic heavy-ion collisions. Annu Rev Nucl Part Sci 49:529–579
10. Heinz U, Kolb P (2002) Two RHIC puzzles: Early thermalization and the HBT problem. http://arxiv.org/abs/hep-ph/?0204061
11. Lednický R, Lyuboshitz VL (1983) Interference correlations of identical particles in models with closely spaced sources. Yad Fiz 38:251–260
12. López Noriega M (for the STAR Collaboration) (2003) Identical particle interferometry at STAR. Nucl Phys A 715:623c–626c
13. Makhlin AN, Sinyukov YuM (1988) The hydrodynamics of hadron matter under a pion interferometric microscope. Z Physics C 39:69–75
14. Pratt S (1984) Pion interferometry for exploding sources. Phys Rev Lett 53:1219–1221
15. Pratt S, Csörgő T, Zimanyi J (1990) Detailed predictions for two pion correlations in ultrarelativistic heavy ion collisions. Phys Rev C 42:2646–2652
16. Retière F, Lisa MA (2003) Observable implications of geometrical and dynamical aspects of freeze-out in heavy ion collisions. http://arxiv.org/abs/nucl-th/?0312024
17. Sinyukov YuM, Lednický R, Akkelin SV, Pluta J, Erazmus B (1998) Coulomb corrections for interferometry analysis of expanding hadron systems. Phys Lett B 432:248–257
18. Tomášik B, Wiedemann UA, Heinz U (2000) Dynamics and sizes of the fireball at freeze-out. Nucl Phys A 663:753–756
19. Wiedemann U, Scotto P, Heinz U (1996) Transverse momentum dependence of Hanbury-Brown-Twiss correlation radii. Phys Rev C 53:918–931